VERTICAL STRUCTURE IN THE MARINE ATMOSPHERIC BOUNDARY LAYER AND ITS IMPLICATION FOR THE INERTIAL DISSIPATION METHOD

ANNA SJÖBLOM* and ANN-SOFI SMEDMAN

Department of Earth Sciences, Meteorology, Uppsala University, Villavägen 16, SE-752 36 Uppsala, Sweden

(Received in final form 14 October 2002)

Abstract. The structure of the marine atmospheric boundary layer and the validity of Monin–Obukhov similarity theory over the sea have been investigated using long term measurements. Three levels of turbulence measurements (at 10 m, 18 m and 26 m) at Östergarnsholm in the middle of the Baltic Sea have been analysed. The results show that turbulent parameters have a strong dependence on the actual height due to wave influence. The wind profile and thus the normalised wind gradient are very sensitive to wave state. The lower part of the boundary layer can be divided into three height layers, a wave influenced layer close to the surface, a transition layer and an undisturbed 'ordinary' surface layer; the depth of the layers is determined by the wave state. This height structure can, however, not be found for the normalised dissipation, which is only a function of the stability, except during pronounced swell where the actual height also has to be accounted for. The results have implications for the height variation of the turbulent kinetic energy (TKE) budget. Thus, the imbalance between production and dissipation will also vary with height according to the variation of wave state. This, in turn, will of course have strong implications for the inertial dissipation method, in which a parameterisation of the TKE budget is used.

Keywords: Inertial dissipation method, Marine atmospheric boundary layer, Turbulent kinetic energy budget, Vertical structure, Waves.

1. Introduction

The atmospheric boundary layer over the sea is in many ways very different from the boundary layer over land, the most obvious difference at the lower boundary being that the sea surface is mobile due to the presence of waves. In atmospheric models used for weather prediction and climate modelling, it is usually assumed that Monin–Obukhov similarity theory (hereinafter referred to as MO-theory) is valid and that expressions found over land for turbulent parameters also are valid over the sea. The influence of waves can, however, modify the structure of the whole marine boundary layer, thereby questioning the validity of MO-theory.

A common way to describe wave-field development, is to use the so-called 'wave age', which is defined as

$$\text{Wave age} = c_0/(U_{10}\cos\theta), \tag{1}$$

* E-mail: Anna.Sjoblom@met.uu.se

Boundary-Layer Meteorology **109:** 1–25, 2003.

where c_0 is the phase velocity of the waves at the peak of the spectrum, U_{10} the wind speed at 10 m and θ the angle between wind and wave directions. Swell, i.e., waves travelling faster than the wind, is here defined as $c_0/(U_{10}\cos\theta) > 1.2$ (Pierson and Moskowitz, 1964).

The atmospheric layer where waves play an important role is usually called the wave boundary layer (WBL), and as Edson and Fairall (1998) showed, as long as the measurements are performed above the WBL, MO-theory can still be used. How to determine the height of the WBL is, however, not perfectly clear. Normally the WBL is just loosely determined as the height below which a wave influence can be seen in the measurements, and most often it is the stress estimates that are used (e.g., Smedman et al., 1994; Edson and Fairall, 1998). Drennan et al. (1999) give an overview of estimates of the WBL height using the stress as the determining parameter. The conclusion is that for a growing sea, the wave influence seems to be of the order of a few metres or less than a metre, but they also give examples of swell cases where the wave influence could be seen through the whole boundary layer (e.g., Smedman et al., 1994).

However, Wilczak et al. (1999) argue that using stress as the determining parameter tends to underestimate the WBL height and that the pressure flux should be used instead, since a wave influence on the pressure flux can be seen at higher heights than the stress influence.

During swell, it is not uncommon to experience very small values of momentum flux (e.g., Smedman et al., 1999), or that momentum is being transported upwards (Grachev and Fairall, 2001). Swell is associated with low or moderate wind speeds, but Rutgersson et al. (2001) show that swell occurs over the Baltic Sea about 40% of the time, so this is not a rare phenomenon.

The structure of the boundary layer also has strong implications on the turbulent kinetic energy (TKE) budget. The budget has been quite thoroughly investigated over land (e.g., Wyngaard and Coté, 1971; Lenschow, 1974; Högström, 1990), but over sea the experiments are more sparse (e.g., Edson and Fairall, 1998; Wilczak, 1999; Sjöblom and Smedman, 2002). The parameterisation of the TKE budget is crucial for the so-called inertial dissipation method, which is widely used as a method to determine fluxes over the sea (e.g., Fairall and Larsen, 1986; Yelland and Taylor, 1996). Most often the measurements are performed at one height, assuming the turbulent fluxes to be constant with height, i.e., assuming validity of MO-theory.

The current investigation is a study of the turbulent structure in the boundary layer over sea and its implications for the TKE budget and the inertial dissipation method. Long term measurements with more than 1300 30-min averages, where more than 700 also contain wave information, have been used. The measurements are taken at an air-sea interaction station situated at the small island of Östergarnsholm in the middle of the Baltic Sea. In Smedman et al. (1999) it was concluded that the flux measurements are likely to represent open sea conditions for most cases with air blowing from the sea sector (see Section 2.1).

Most of the swell encountered at Östergarnsholm is produced in the southern part of the Baltic Sea and then propagated northwards. Since the Baltic Sea is semi-enclosed, the swell has a tendency to be more unidirectional (e.g., Sjöblom and Smedman, 2002; hereinafter referred to as SS 2002), and it also has a smaller amplitude than that usually observed in the open ocean. It must therefore be kept in mind that the conditions concerning the effect of swell may be different for the open ocean.

Section 2 describes the measurements and the data used. The wave influence on the atmospheric boundary layer and MO-theory is discussed in Section 3 and its implications for the TKE budget and the inertial dissipation method in Section 4. Section 5 presents a case study of two days in August 1996, and the results are finally discussed in Section 6 with references to previous studies.

2. Measurements and Data

2.1. Measurements

The measurements are performed at the island of Östergarnsholm, outside Gotland in the middle of the Baltic Sea (Figure 1). Here, measurements have been performed on a 30-m tower semi-continuously since May 1995.

Turbulence instruments (Solent Ultrasonic Anemometer 1012R2, Gill Instruments, Lymington, United Kingdom) are placed at 9, 17 and 25 m above the tower base and data recorded at 20 Hz. Slow response (‘profile’) instruments are placed at five heights on the tower, at 7, 12, 14, 20 and 29 m above the tower base, measuring wind speed, wind direction and temperature at 1 Hz.

Both turbulence and profile instruments have been individually calibrated in a large wind tunnel before installation on the tower. The calibration procedure for the turbulence instruments follows that of Grelle and Lindroth (1994), where the flow distortion made by the instrument itself is taken into account in a calibration matrix. From this the three wind components are obtained. The heat flux measured by the sonic anemometer is close to the virtual heat flux, $\overline{w'\theta_v'}$ (SS 2002), defined as

$$\overline{w'\theta_v'} = \overline{w'\theta'} + 0.61\theta\overline{w'q'}, \tag{2}$$

where θ is the potential temperature and q the specific humidity. $\overline{w'\theta_v'}$ has been corrected for ‘cross-wind’ velocity contamination according to Kaimal and Gaynor (1991). However, this correction is based on a vertical orientation of the sonic temperature sensor, which is not the case for the sonic used here. How large an error this difference gives is not clear, but it has been shown that the results are substantially improved when the correction is applied (C. Johansson, 2002, personal communication).

The tower stands on the southernmost tip of the island and the distance to the shoreline is normally a few tens of metres. The height between the tower base and the water surface varies due to varying sea level. The height variation is about 0.7 m, giving averaged heights to the turbulence instruments of 10.4, 17.9 and 26.4 m. The sea-level measurements are performed at the west coast of Gotland in Visby harbour, and have been recalculated to fit the Östergarnsholm data using a calibration procedure described in SS 2002. Since the measuring heights vary, the three heights will hereinafter be referred to as Level 1 (about 10 m), Level 2 (about 18 m) and Level 3 (about 26 m).

Only waves close to the island (order of 20 m) shoal, even during high wind speed conditions. A flux footprint analysis performed in Smedman et al. (1999) shows that during neutral conditions, about 70% of the fluxes measured at approximately 10 m height originate from areas between 250 and 1700 m upwind. For the measurements at approximately 26 m the upwind distance is instead 770–5300 m. During unstable conditions, the fluxes originate from areas closer to the island (about 90% originates from beyond 100 m), but the areas are still well beyond the shoaling zone.

The sea-floor slope outside the island is approximately 1 : 30 at 500 m from the shore, and about 10 km from the peninsula the water depth is about 50 m, becoming greater than 100 m further out. This permits an undisturbed wave field for most conditions encountered, and as was concluded in Smedman et al. (1999), the shallow water effect on the turbulence structure in the atmosphere seems small. However, during high wind speeds, a correction for limited water depth has to be applied to the phase velocity of the waves at the peak of the spectrum, c_0. Only measurements in the sector 100°–220° are used in this study; in this sector, there is an undisturbed fetch over water (more than 150 km). In the upwind area a Wave-Rider Buoy (owned and operated by the Finnish Institute for Marine Research) is deployed about 4 km from Östergarnsholm (direction 115°, Figure 1), thereby representing the wave conditions in the 'footprint area' outside Östergarnsholm. The wave measurements have been performed semi-continuously during the same period as the tower measurements with the exception of wintertime periods with risk of ice damage.

The buoy is moored at 36 m water depth, measuring sea surface (bucket) temperature, significant wave height, wave direction and the energy spectra of the wave field. Wave data are recorded once an hour. The directional spectrum is calculated from 1600 s of data onboard the buoy. The spectrum has 64 frequency bands (0.025–0.58 Hz). The significant wave height is calculated by a trapezoidal method from frequency bands 0.05–0.58 Hz, and the peak frequency is determined by a parabolic fit (Smedman et al., 1999).

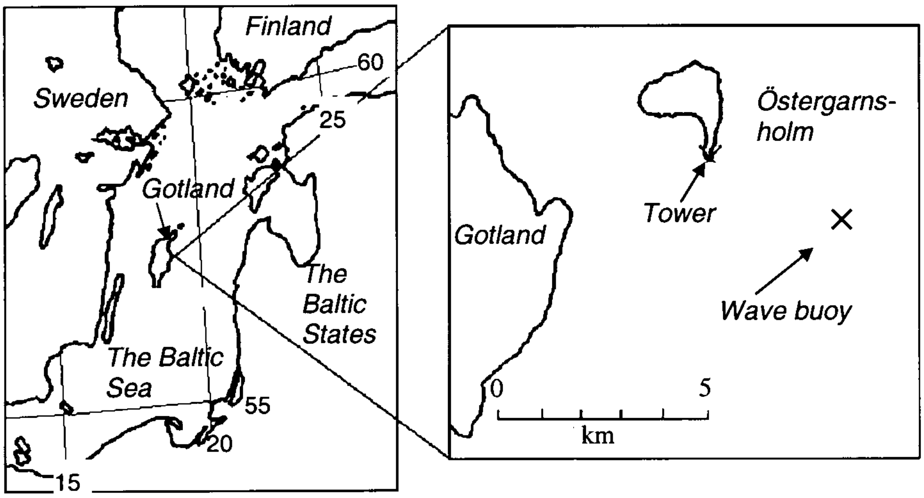

Figure 1. Map of the Baltic Sea, with a close up of Östergarnsholm. The location of the wave buoy is also indicated.

2.2. Data

The measurements used were taken within the period May 1995–December 1997, and the data set consists only of data with long overwater fetch. 30-min averages have been used both for the turbulence and the profile measurements; wave data were available once an hour. Wave data were unfortunately not available for all the tower measurements and, in addition, data with more than 80° angle between wind and wave directions have been removed from the data set, since at 90° the wave age goes to infinity (Equation (1)) and for larger angles it becomes negative. The data show hardly any dependence on the choice of this angle; using, for example, an angle of 40°, where the waves and the wind are more aligned, does not change the results significantly.

The numbers of 30-min averages at the three levels are: 2166 at Level 1 (SS 2002), 1351 at Level 2, and 1607 at Level 3. Of these data, wave data are available for: 1033 data points at Level 1 (SS 2002), 741 at Level 2, and 888 at Level 3. All calculated properties have been determined locally, and wind speed ranges from 2 to about 20 m s^{-1}. The stability varies from very unstable to very stable, but about 90% of the data is in the near-neutral range, i.e., $|z/L| < 0.5$, where the stability parameter z/L is defined as

$$\frac{z}{L} = -\frac{zgk\overline{w'\theta_v'}}{u_*^3 T_0}, \tag{3}$$

where L is the Monin–Obukhov length, z the measurement height, g the acceleration due to gravity, k the von Karman constant taken as 0.40 (Högström, 1996), $\overline{w'\theta_v'}$ the virtual heat flux (Equation (2)), u_* the friction velocity and T_0 a reference temperature in the surface layer.

The wind gradient was derived using a third-order polynomial from a best fit to the log-lin plot of wind speed measurements from the five cup anemometers. The gradient has then been calculated at the heights of the turbulence measurements. The third-order fit was chosen in order to achieve a good fit to the actually measured wind profiles (see also Section 3b). Data with wind speeds less than 2 m s^{-1} have been removed due to statistical uncertainties, and the data have also been subjectively checked for large variations over a small time scale, thereby removing data during frontal passages, etc. Allowing such low wind speeds questions the assumption of stationary conditions. But, since most of the swell cases have wind speeds between 2 and 5 m s^{-1}, all the profiles and the fitted curves have been manually checked, and those cases where stationarity could be in doubt have been removed. This seemed to be a preferable method, since using, for example, 4 or 5 m s^{-1} as a lower threshold, most of the swell data will be removed, and a study of wave influence would become much more difficult.

The terms in the TKE budget have been determined directly from the measurements except for the pressure transport term, which was determined as a residual. The dissipation was calculated from manually checked spectra of longitudinal wind velocity. If the slope in the inertial subrange of $nS_u(n)$ was approximately $-2/3$, where n is the frequency and $S_u(n)$ the spectral density, a log-log fit of the values in the inertial subrange was performed, and values of $nS_u(n)$ and frequency n were calculated from this curve. Spectra that did not fulfil the above requirements have been rejected. The dissipation, ϵ could then be determined from

$$\epsilon = \left(\frac{nS_u(n)}{\alpha}\right)^{3/2}\left(\frac{2\pi n}{U}\right), \tag{4}$$

by assuming Kolmogorov similarity and applying Taylor's hypothesis. Here, U is the mean velocity, and α the Kolmogorov constant, which has been set equal to 0.52 following Högström (1996).

3. Wave Influence on the Marine Atmospheric Boundary Layer

As discussed in the introduction, the marine atmospheric boundary layer is often influenced by waves. The waves can be characterised as three types of waves, depending on the wave age (Equation (1)):

- Growing waves, $c_0/(U_{10}\cos\theta) < W_{\mathrm{grow}}$,
- Mature or saturated waves, $W_{\mathrm{grow}} < c_0/(U_{10}\cos\theta) < 1.2$,
- Swell, $c_0/(U_{10}\cos\theta) > 1.2$.

The precise value of W_{grow} that separates growing waves from mature waves is not completely clear, but the value is somewhere between 0.5 and 0.9 (e.g., Dobson, 1994; Drennan, 1999; SS 2002).

3.1. MONIN-OBUKHOV SIMILARITY THEORY

According to Monin–Obukhov similarity theory (e.g., Obukhov, 1971), normalised turbulence parameters in the lower part ($\approx$10%) of the boundary layer (known as the surface layer), which is characterised by approximately constant fluxes of momentum and heat, can be uniquely described by the following four parameters: g/T_0, $\overline{w'\theta'_v}$, u_* and z, where g/T_0 is the buoyancy parameter. For example, the normalised wind gradient, ϕ_m, will then be a unique function of stability (Equation (3)),

$$\frac{\partial U}{\partial z}\frac{kz}{u_*} = \phi_m\left(\frac{z}{L}\right). \tag{5}$$

3.2. CONNECTION BETWEEN WAVES AND ATMOSPHERIC STABILITY

The total surface stress, τ, in the marine atmospheric boundary layer can be divided into three parts

$$\tau = \tau_{\text{turb}} + \tau_{\text{wave}} + \tau_{\text{visc}}, \tag{6}$$

where τ_{turb} is the turbulent shear stress, τ_{wave} the wave induced stress and τ_{visc} the viscous stress. For large wave ages (Equation (1)), τ_{wave} will be small and for some occasions even negative. The total surface stress will therefore be reduced and give a lower value of the friction velocity, u_*, defined as

$$u_*^2 = [(-\overline{u'w'})^2 + (-\overline{v'w'})^2]^{1/2} = \frac{|\tau|}{\rho}, \tag{7}$$

where $\overline{u'w'}$ and $\overline{v'w'}$ are the components of the kinematic momentum flux in the alongwind and crosswind directions. The small u_* value during swell will in turn result in a large value of $|z/L|$ (Equation (3)).

Thus, because the Monin–Obukhov length depends in part on the surface wind stress, and because the surface wind stress is dependent in part on both swell and wind seas, the swell will have an influence on the computation of atmospheric stratification. The connection between stability and the wave age is therefore very close, especially during swell conditions.

3.3. THE WAVE BOUNDARY LAYER

As discussed in the introduction, the wave boundary layer (WBL) is usually defined as the atmospheric layer where waves influence the turbulent structure. Above the WBL MO-theory is supposed to be valid, but in the WBL an additional parameter must be added describing the influence of waves.

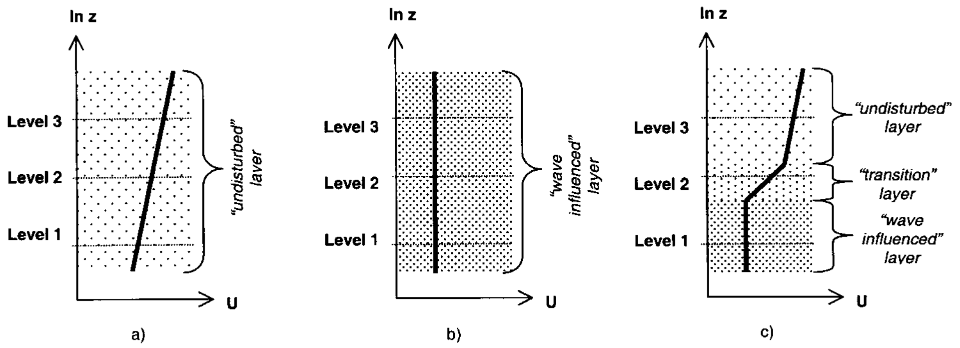

Figure 2. Typical appearance of near-neutral wind profiles over the sea: (a) Growing sea, (b) strong swell, (c) the transition phase between growing sea and strong swell.

3.3.1. *The Wind Profile*

The wind profile over sea is very dependent on the wave state. Figure 2 shows three examples (schematically) of a wind profile during neutral conditions. For growing sea, i.e., $c_0/(U_{10}\cos\theta) < 0.5$, the wind profile is logarithmic (Figure 2a) and similar to wind profiles over land. The wave influenced layer is now very shallow (see discussion above) and is situated below the lowest measuring height, i.e., all three measuring levels are 'undisturbed'.

During swell when the waves are moving faster than the wind, it is not uncommon that a 'wave driven wind' appears (e.g., Smedman et al., 1999). If the swell is strong, this wave influenced layer can reach considerable heights and measurements at all three levels will now be in the 'wave influenced' layer (Figure 2b) having a small or perhaps even negative gradient $\partial U/\partial z$.

However, when the wave age increases from a growing sea, the wind profile does not momentarily change from (a) to (b), and there is often a transition phase in between. The waves will start to influence the wind profile for $c_0/(U_{10}\cos\theta) > 0.5$, and a typical appearance of the wind profile (schematically) is shown in Figure 2c. The wind profile can now be divided into three layers: A higher undisturbed 'ordinary' surface layer (as in Figure 2a), a lower 'wave influenced' layer (as in Figure 2b), and in between a 'transition' layer is situated. This layer is indirectly influenced by the waves, and the wind gradient $\partial U/\partial z$ will therefore be larger than in the 'wave influenced' layer or the 'undisturbed' layer.

The analysis of the wind profile shows that the schematical shape in Figure 2c with three layers is very common for $c_0/(U_{10}\cos\theta) > 0.5$. This means that the wind profile is not only influenced by a fully developed swell; the influence already exists for mature or saturated waves. It is also common that the three measuring levels are situated one in each layer, i.e., Level 1 in the 'wave influenced' layer, Level 2 in the 'transition' layer and Level 3 in the undisturbed 'ordinary' surface layer.

This will of course have strong implications for the normalised wind gradient, ϕ_m, but this will be further discussed in Section 3.4.1.

3.3.2. *Constant Flux Layer*

Because of the wave influence, it is a difficult problem to determine whether all three measuring heights are within the surface layer. A common definition of the surface layer is the lowest 10% of the boundary layer. But unfortunately, no boundary-layer height measurements were available for this data set. The surface layer can also be defined as the layer where the turbulent fluxes vary no more than 10%. Within the surface layer, MO scaling (Section 3a) is assumed to be valid, and the structure of the turbulence should scale with the height above ground, z.

Table I shows averaged values of the normalised difference of the kinematic momentum flux in the along-wind direction, $\overline{u'w'}$, at the three levels, for different stability and wind speed ranges. For $-0.2 < z/L < 0.2$ the difference is within 10% for both high and low wind speeds, which then indicates that all three levels are within the surface layer. The difference on the stable and the unstable side within this range is negligible.

For unstable conditions ($-2.0 < z/L < -0.2$), where swell is almost always present (see Section 3.2), the ratios are much larger, especially for Level 3/Level 1, i.e., there is no constant turbulent flux layer. But as discussed earlier, an additional parameter should be used in the WBL, describing the wave influence.

For stable conditions ($z/L > 0.2$), the difference is again larger than 10%, but the surface layer is probably very shallow here and it is likely that both Levels 2 and 3 are above the surface layer.

The height variation of the heat flux, $\overline{w'\theta_v'}$, could also be used to determine the surface-layer height. But over the sea $\overline{w'\theta_v'}$ is often very small, and subsequently, the scatter in normalised values becomes large and the result very uncertain.

3.4. Implications of Wave Influence for Monin–Obukhov Similarity Theory

The relationships in Section 3.1 have been developed over land, but the question is if MO-theory is valid over the sea, where the roughness elements consists of moving waves. Two ways to verify this will be discussed below.

3.4.1. *The Normalised Wind Gradient ϕ_m*

The normalised wind gradient, ϕ_m (Equation (5)), can also be defined as

$$\phi_m = -\frac{kz}{u_*^3}\left(\overline{u'w'}\frac{\partial U}{\partial z} + \overline{v'w'}\frac{\partial V}{\partial z}\right). \tag{8}$$

As shown in SS 2002, Equation (8) can be simplified for this data set to

$$\phi_m = -\frac{kz}{u_*^3}\overline{u'w'}\frac{\partial U}{\partial z}. \tag{9}$$

TABLE I

Ratio of $\overline{u'w'}$ from the three levels: L1 = Level 1, L2 = Level 2 and L3 = Level 3.

Ratio of $\overline{u'w'}$	$-2 < z/L < -0.2$	$-0.2 < z/L < 0.2$	$-0.2 < z/L < 0.2$ $U < 10$ m s^{-1}	$-0.2 < z/L < 0.2$ $U > 10$ m s^{-1}	$z/L > 0.2$
(L2 − L1)/L1	0.51	0.05	0.07	0.04	0.20
(L3 − L1)/L1	0.61	0.06	0.07	0.08	0.44
(L3 − L2)/L2	0.24	0.04	0.04	0.06	0.13
Number of data	103	804	428	255	8

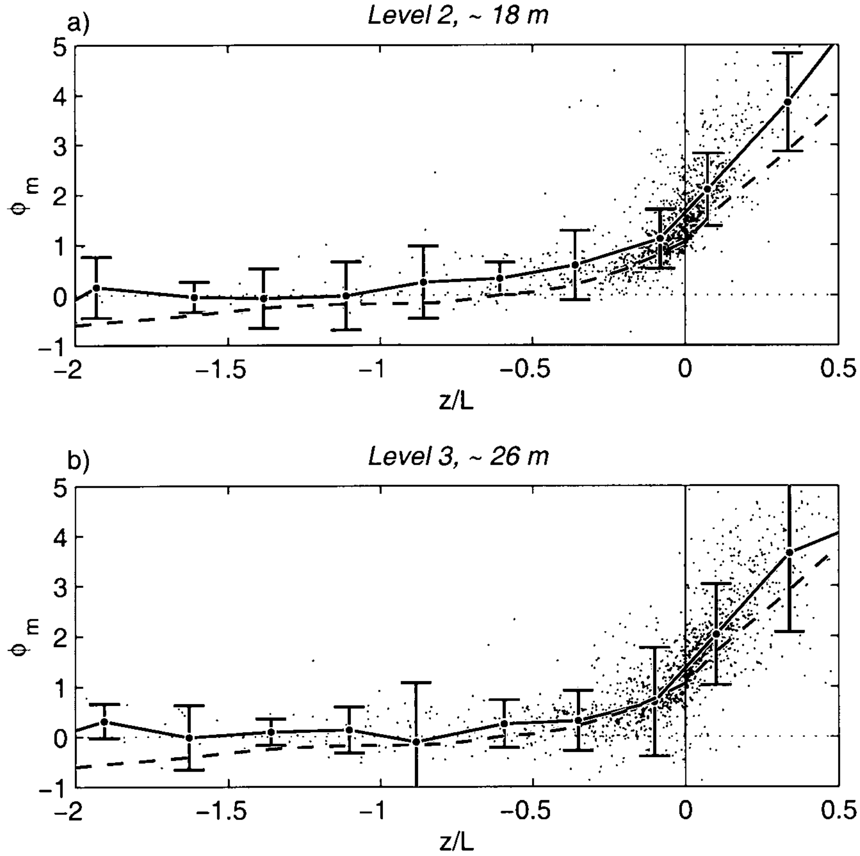

Figure 3. Normalised wind gradient, ϕ_m, as a function of stability: (a) Level 2 (≈18 m), (b) Level 3 (≈26 m). Dots are all measurements, the thick solid line (—) the averaged curve, and the filled circles (●) are the bin-averaged values. Dashed line (- - -) is the averaged results from Level 1 (≈10 m, after Sjöblom and Smedman, 2002).

Figure 3 shows ϕ_m as a function of the stability z/L (Equation (5)); Figure 3a shows Level 2 and Figure 3b Level 3. All variables (i.e., u_*, $\partial U/\partial z$ and $\overline{u'w'}$) have been determined locally at the three heights. Dots are all measurements, the solid line the averaged curve, and the filled circles the bin-averaged values with standard deviations. The dashed line is after SS 2002, showing averaged results from Level 1.

There are not as many negative values of ϕ_m during unstable conditions ($z/L < -0.5$) at Levels 2 and 3 as was found for Level 1. Swell will almost always influence at these stabilities and it is obvious that Level 1 is mostly affected, thereby giving negative gradients (cf. Figure 2) and also negative values of ϕ_m.

On the stable side ($z/L > 0$) ϕ_m increases rapidly and Levels 2 and 3 both give slightly higher values than Level 1. However, as discussed earlier, it might be questioned if Levels 2 and 3 really are in the surface layer for the most stable cases.

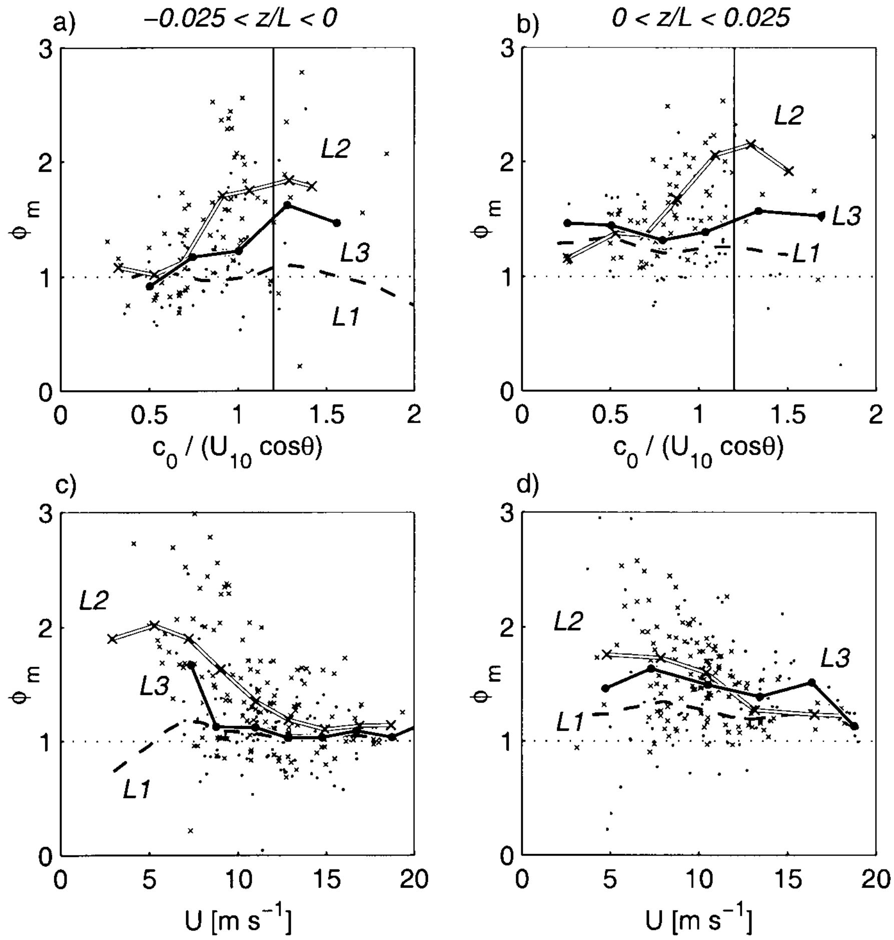

Figure 4. Near-neutral values of the normalised wind gradient, ϕ_m, at three levels. Dots are measurements at Level 2 and crosses $(\times)$ at Level 3; double line (=) is the averaged curve at Level 2, and dash-dotted (●—●) at Level 3. Dashed line (- -) is an averaged curve from Level 1 (after Sjöblom and Smedman, 2002): (a) Slightly unstable data, $-0.025 < z/L < 0$ as a function of $c_0/(U_{10}\cos\theta)$, (b) slightly stable data, $0 < z/L < 0.025$ as a function of $c_0/(U_{10}\cos\theta)$, (c) slightly unstable data, $-0.025 < z/L < 0$ as a function of wind speed, (d) slightly stable data, $0 < z/L < 0.025$ as a function of wind speed.

Although the scatter is large, the mean curve for Level 2 shows that $\phi_m > 1.0$ at neutral stability, while at Level 3 it is close to 1.0.

In Figure 4 the near-neutral ϕ_m values are plotted as a function of wave age and wind speed. Dots are measurements at Level 2 and crosses at Level 3. The dashed line is the averaged result from Level 1 (after SS 2002), the double line Level 2, and the dash-dotted line Level 3.

In Figure 4a, where ϕ_m is plotted as a function of wave age ($c_0/(U_{10}\cos\theta)$) for slightly unstable stratification, it is clear that ϕ_m is close to 1.0 for a growing sea

($c_0/(U_{10}\cos\theta) < 0.6$). But as shown in Figure 4b, this is not the case on the stable side; ϕ_m is here rather around 1.3 at all levels for growing sea. Thus, ϕ_m increases rapidly with increasing stability, which was also seen in Figure 3.

This result for a growing sea corresponds well to high wind speeds ($U > 12$ m s^{-1}), which is seen in Figure 4c, where ϕ_m on the unstable side is plotted as a function of wind speed, and in Figure 4d on the stable side.

For mature waves and swell ($c_0/(U_{10}\cos\theta) > 0.6$), ϕ_m is no longer constant with height. Especially ϕ_m at Level 2 increases rapidly while Level 1 is close to 1.0 (Figure 4a). This can also been seen in Figure 4c for $U < 12$ m s^{-1}.

The reason for the high ϕ_m values, especially at Level 2, is probably that this level is often situated in the 'transition' layer (cf. Figure 2), where the gradient is large. It is also clear from Figure 4, that this transition layer does not only exist for swell conditions ($c_0/(U_{10}\cos\theta) > 1.2$) or low wind speeds, but starts to form already for mature or saturated waves ($c_0/(U_{10}\cos\theta) \approx 0.6$). ϕ_m now becomes a function of both stability and height itself.

The conclusion for mature waves and swell is that we do not have a constant turbulent flux layer and MO-theory can therefore not be used.

3.4.2. *Height Variations of the Inertial Subrange*

If MO scaling can be applied over the sea, the inertial subrange of wind spectra should scale with height within the surface layer. The normalised dissipation, ϕ_ϵ which is determined from the inertial subrange (Equation (4)), should therefore be only a function of stability, z/L, and not have a dependence on the height itself; here, ϕ_ϵ is defined as

$$\phi_\epsilon = \frac{\epsilon k z}{u_*^3}. \tag{10}$$

In Figure 5, ϕ_ϵ is plotted as a function of stability, z/L (symbols as in Figure 3). For $|z/L| < 0.5$, ϕ_ϵ is dependent only on the stability z/L, and is close in magnitude for all three levels. A minimum of ϕ_ϵ is found at $z/L \approx -0.25$ for all levels, which agrees with other studies both over the sea and over land (e.g., Schacher et al., 1981; Högström, 1990).

However, if only near-neutral data are plotted as a function of wave age (Figure 6a, $-0.025 < z/L < 0$; Figure 6b, $0 < z/L < 0.025$; symbols as in Figure 4) the height constancy of ϕ_ϵ is only evident for $c_0/(U_{10}\cos\theta) < 0.9$. At larger wave ages the three levels start to deviate, i.e., ϵ does not scale with height any more. For swell, ϕ_ϵ becomes large, especially at Level 2.

For $z/L < -0.5$ Level 2 and Level 3 have smaller values than Level 1, i.e., ϕ_ϵ is not only a function of z/L but also has a dependence on height itself.

Thus, contrary to ϕ_m, the transition layer (Figure 2c) does not influence ϕ_ϵ below $c_0/(U_{10}\cos\theta) \approx 0.9$. It can therefore be concluded that ϕ_ϵ is a function of z/L only, and not dependent on the actual measurement height, for near-neutral conditions and $c_0/(U_{10}\cos\theta) < 0.9$, i.e., MO scaling holds true for $c_0/(U_{10}\cos\theta) < 0.9$

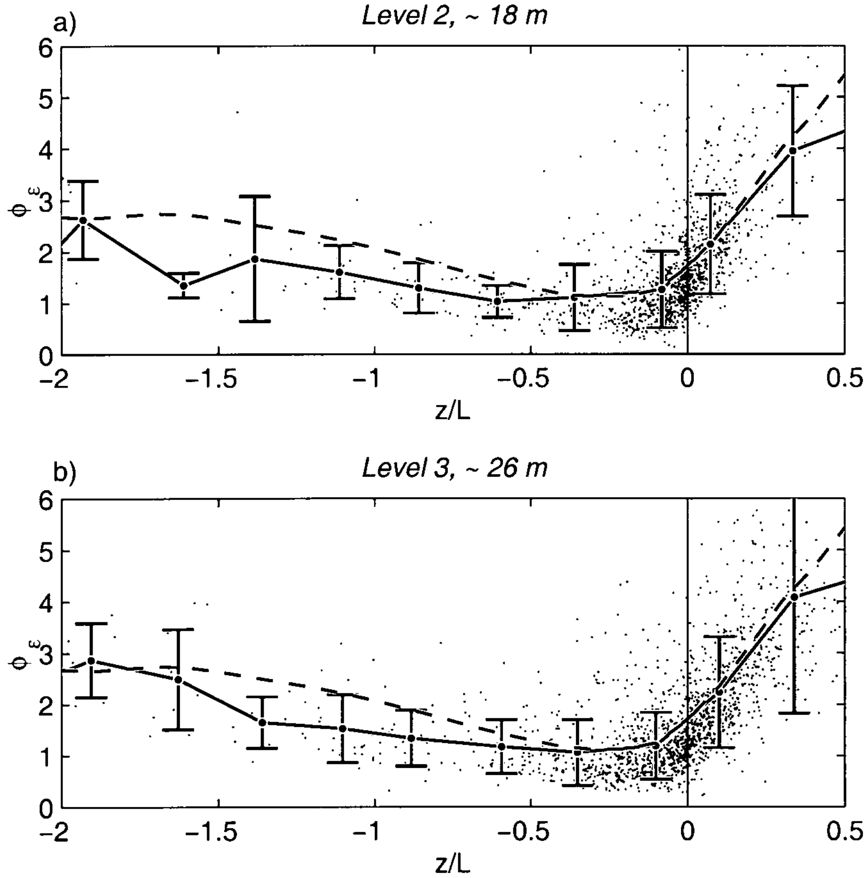

Figure 5. Normalised dissipation, ϕ_ϵ, as a function of stability: (a) Level 2 (≈18 m), (b) Level 3 (≈26 m). Symbols as in Figure 3.

at all levels, when these measurements are within the surface layer. But, for $c_0/(U_{10}\cos\theta) > 0.9$ this is not the case. Here, the conditions resemble that of very unstable conditions, and the inertial subrange should rather scale with the height of the boundary layer (Smedman et al., 1999).

4. The Turbulent Kinetic Energy Budget and the Inertial Dissipation Method

The turbulent structure of the marine boundary layer will also affect the turbulent kinetic energy budget. The TKE budget provides a description of the physical processes that generate turbulence and the budget also plays a fundamental role in the so-called inertial dissipation method. The TKE budget at Level 1 was thoroughly described in SS 2002, but based on the results in Section 3, it is not obvious

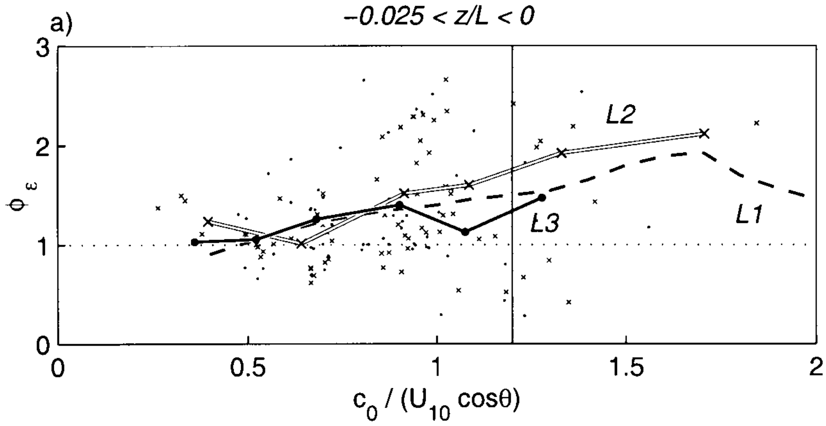

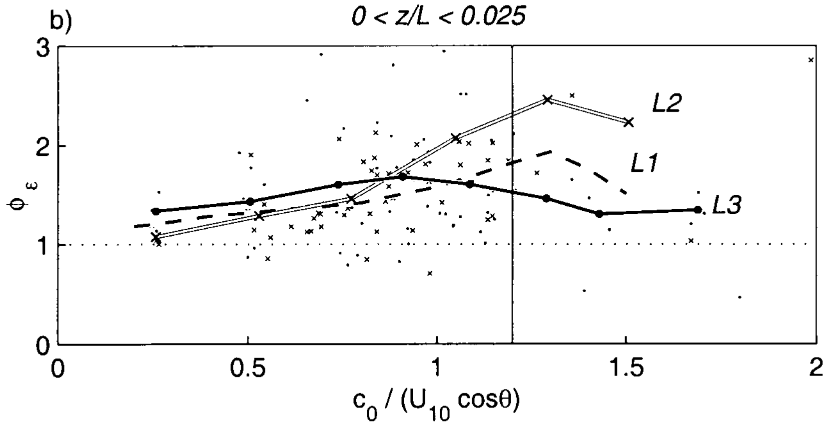

Figure 6. Near-neutral values of the normalised dissipation, ϕ_ϵ, at three levels as a function of wave age. Symbols as in Figure 4: (a) Slightly unstable data, $-0.025 < z/L < 0$, (b) slightly stable data, $0 < z/L < 0.025$.

that these results are valid throughout the whole surface layer. This will now be discussed in detail.

4.1. Theory

The normalised turbulent kinetic energy budget during stationary and horizontally homogeneous conditions is defined as

$$\underset{\text{(I)}}{\frac{kz}{u_*^3}\left(\overline{u'w'}\frac{\partial\overline{u}}{\partial z}+\overline{v'w'}\frac{\partial\overline{v}}{\partial z}\right)}-\underset{\text{(II)}}{\frac{kz}{u_*^3}\frac{g}{T_0}\overline{w'\theta_v'}}+\underset{\text{(III)}}{\frac{kz}{u_*^3}\frac{\partial\overline{w'e}}{\partial z}}+\underset{\text{(IV)}}{\frac{kz}{u_*^3}\frac{1}{\rho}\frac{\partial\overline{p'w'}}{\partial z}}+\underset{\text{(V)}}{\frac{kz}{u_*^3}\epsilon}=0, \qquad (11)$$

where $e = 0.5(u'^2 + v'^2 + w'^2)$ and ρ is the air density. Term I corresponds to the normalised mechanical production of TKE from the mean flow, II to the normalised buoyant production or loss, (III) to the normalised turbulent transport, (IV) to the normalised pressure transport and (V) to the normalised molecular dissipation of TKE. Equation (11) is the same as

$$\underset{\text{(I)}}{\phi_m} - \underset{\text{(II)}}{\frac{z}{L}} - \underset{\text{(III)}}{\phi_t} - \underset{\text{(IV)}}{\phi_p} - \underset{\text{(V)}}{\phi_\epsilon} = 0. \tag{12}$$

Term I and V were analysed above, and will of course play an important role in the total budget. Term II is by definition the same as the stability (Equation (3)) and will not be discussed any more. The two terms that have not been discussed so far are the two transport terms III and IV. It is common to assume that these are small or self-cancelling, at least in near-neutral conditions. This is the same as assuming that local production equals local dissipation, although, as shown in SS 2002, this assumption can be questioned. Below, a possible dependence on the measuring height of the transport terms is investigated.

4.2. Transport terms in the TKE budget

The transport terms can neither produce nor destroy energy, just re-locate it. The normalised turbulent transport (ϕ_t) was found to be very small compared to the normalised pressure transport (ϕ_p) (not shown here). So the sum of the transport terms, i.e., the imbalance between local production and dissipation, mainly originates from the pressure transport. This is in accordance with, for example, Janssen (1999) who showed that the pressure transport is not negligible, not even in high wind speed conditions. SS 2002 showed that the sum of the transport terms seldom is close to zero at a height of approximately 10 m (Level 1), and that this imbalance is a function of stability, wave age, and to some degree wind speed.

4.3. Implications for the inertial dissipation method

The inertial dissipation method is a preferable method to determine the fluxes over the sea, since it is not so sensitive to platform motion and flow distortion as the eddy-correlation method. However, a correct parameterisation of the terms in the TKE budget is of fundamental importance for the inertial dissipation method. For a description of the method, see, for example, Yelland and Taylor (1996). The question that has been most debated is how to parameterise the imbalance between production and dissipation, which is equal to the sum of the transport terms.

The imbalance is shown in Figure 7, plotted as a function of stability (symbols as in Figure 3); Figure 7a shows Level 2 and Figure 7b shows Level 3.

The dissipation is larger than the production, i.e., a negative imbalance, for near-neutral conditions ($z/L \approx 0$) at Levels 1 and 3. But for Level 2, the imbalance is close to zero. ϕ_m is large at Level 2 (Figure 3a) due to the transition layer and since the imbalance is determined from ϕ_m, z/L and ϕ_ϵ (term I, II and V in Equation

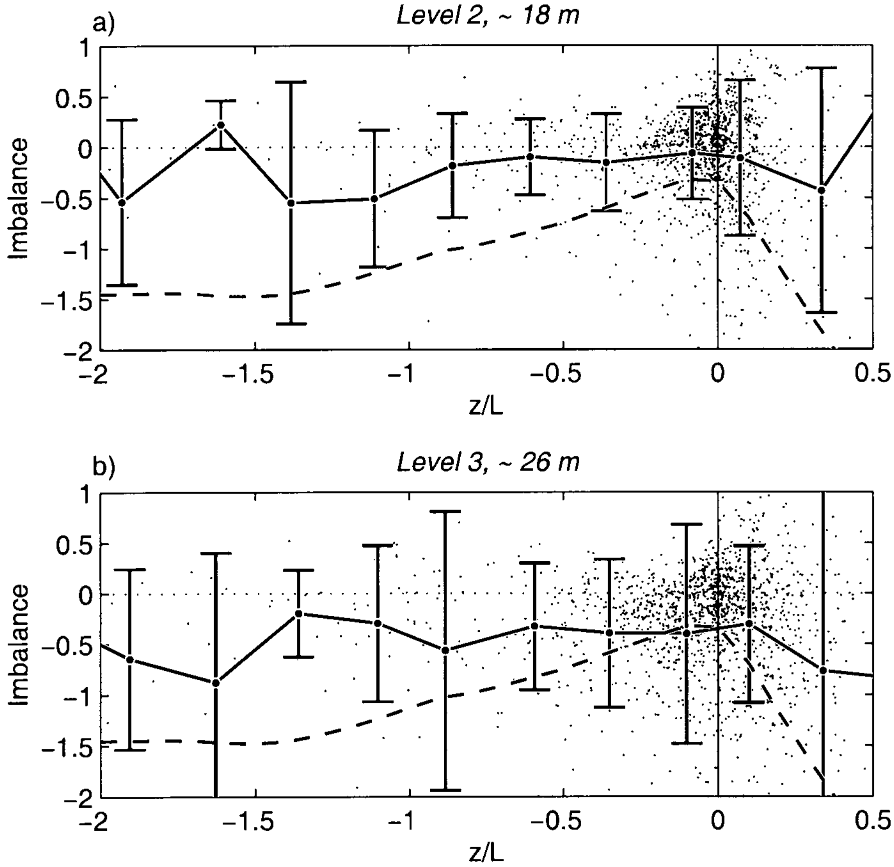

Figure 7. Normalised imbalance (normalised production minus normalised dissipation) as a function of stability: (a) Level 2 ($\approx$18 m), (b) Level 3 ($\approx$26 m). Symbols as in Figure 3.

(11)), this will be reflected in the imbalance. But, it should be remembered that this is a locally determined balance.

For unstable conditions ($z/L < 0$), the imbalance is largest at Level 1; i.e., dissipation is much larger than the production.

Since it has been shown above that some of the terms in the TKE budget have a strong height dependence due to wave state, this will also be the case for the imbalance. This can be seen in Figure 8, where the near-neutral data are plotted as a function of wave age (symbols as in Figure 4). Figure 8a shows $-0.025 < z/L < 0$ and Figure 8b shows $0 < z/L < 0.025$.

The imbalance at Level 1 is positive for a growing sea for both unstable and stable conditions. This was explained in SS 2002 as an input of energy to the growing waves rather than its dissipation into heat (Edson and Fairall, 1998). Levels 2 and 3 only show this behaviour on the stable side. On the unstable side dissipation is somewhat larger than production, i.e., a negative imbalance.

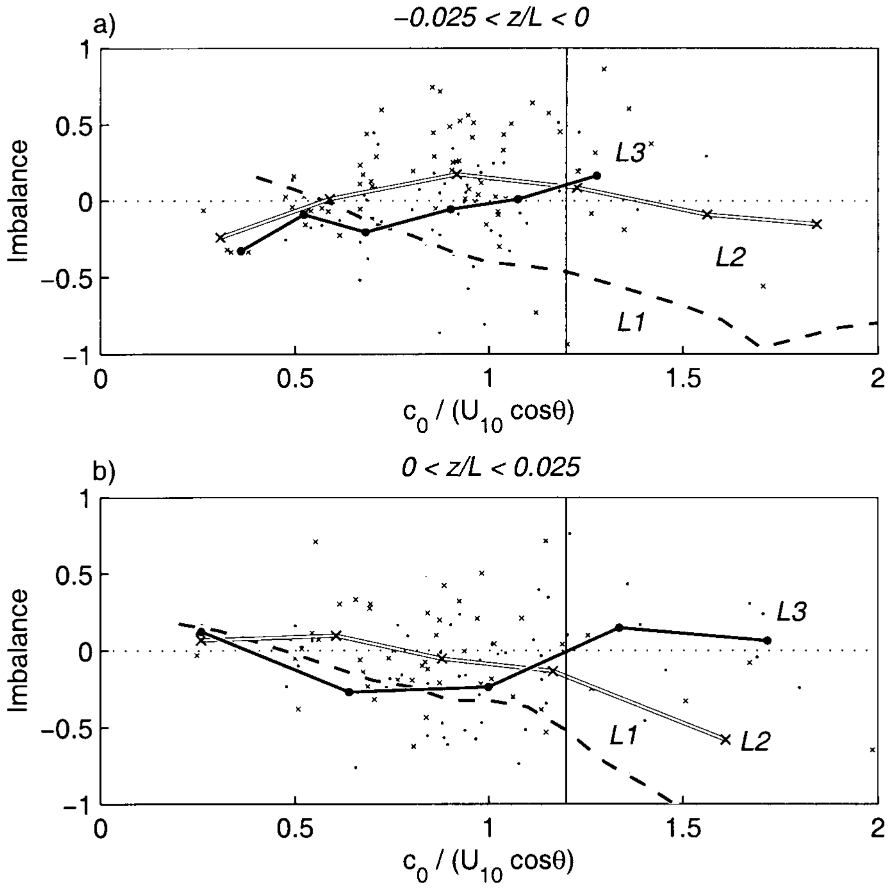

Figure 8. Near-neutral values of the normalised imbalance (normalised production minus normalised dissipation at three levels as a function of wave age. Symbols as in Figure 4: (a) Slightly unstable data $-0.025 < z/L < 0$, (b) slightly stable data, $0 < z/L < 0.025$.

For mature waves and swell, Level 1 has the largest imbalance, dissipation being much larger than the production. For Levels 2 and 3, the behaviour on the unstable and stable side is somewhat different.

The imbalance will of course be different if another value of the Kolmogorov constant, α, is used when calculating the dissipation (Equation (4)). Deacon (1988) suggested that an 'apparent' value could be used in order to compensate for a possible imbalance between normalised production and normalised dissipation. But, as will be shown elsewhere, this 'apparent' value is not a constant, and has a strong dependency on, for example, the wave state.

To conclude, it is not correct to assume that the sum of the transport terms is small, even in near-neutral conditions. Except for the influence of waves, which was thoroughly investigated in SS 2002, this study shows that also the measurement height has to be taken into account when using the inertial dissipation method, and that the imbalance can only be determined locally.

Measurements from a buoy with measuring heights of a few metres will need a completely different parameterisation of the TKE budget than measurements from a ship with measurement heights 10–25 m. The buoy will most likely be in the lowest wave influenced layer, while it is more uncertain in which layer the measurements on a ship are made.

5. Case Study

Two days, 25–26 August 1996, have been chosen for a detailed study of the possible vertical variations of turbulent parameters discussed above, i.e., the normalised wind gradient, ϕ_m, the normalised dissipation, ϕ_ϵ, and the imbalance between normalised production and dissipation.

These two days are characterised by fairly constant wind and wave directions since a high pressure system is situated north-east of Gotland, and controls the wind direction during this period. The wind speed, wave age and stability are shown in Figure 9. The filled circles (●) indicate when measurements were available. The x-axis shows hours from start, which is taken as midnight (0000 LST) August 25.

The wind speed at 10 m (Figure 9a) first increases until 1200 h, with a maximum wind speed of about 10 m s^{-1}. Between 12–20 h it decreases to about 3 m s^{-1}. Then the wind speed increases again to about 10 m s^{-1} during a couple of hours; thereafter it is fairly constant, at about 7–9 m s^{-1}.

The wave age (Figure 9b) follows the wind speed, with low wave age during the increase in wind speed, and swell $c_0/(U_{10} cos\theta) > 1.2$ for the decreasing wind speed. Unfortunately, wave data were not available for all meteorological data, but the trend is quite clear.

The stability determined locally at the three measuring levels (Figure 9c, symbols as in Figure 4) is mostly unstable ($z/L < 0$), even if it is stable ($z/L > 0$) for some measuring points, especially at Level 3 during the swell period. It can therefore be questioned if Level 3 really is in the surface layer during this period.

In Figure 10, the normalised wind gradient, ϕ_m, the normalised dissipation, ϕ_ϵ, and the imbalance between normalised production and dissipation (i.e., the sum of the transport terms) have been plotted as a time series for these two days in August 1996.

Figure 10a shows the normalised wind gradient, ϕ_m (symbols as in Figure 4), where it is obvious that ϕ_m at Level 2 is larger than at the other levels during most of the time, especially during the swell period (12–20 h). This supports the ideas of Section 3.4.1 that Level 2 often is situated in the transition layer for a non-growing sea. Level 3 also gives higher values of ϕ_m than Level 1 during the swell period, but as seen in Figure 9c, z/L is larger than zero at Level 3, so this is not an anomalous result. For the other periods, Levels 1 and 3 are quite close in magnitude. Level

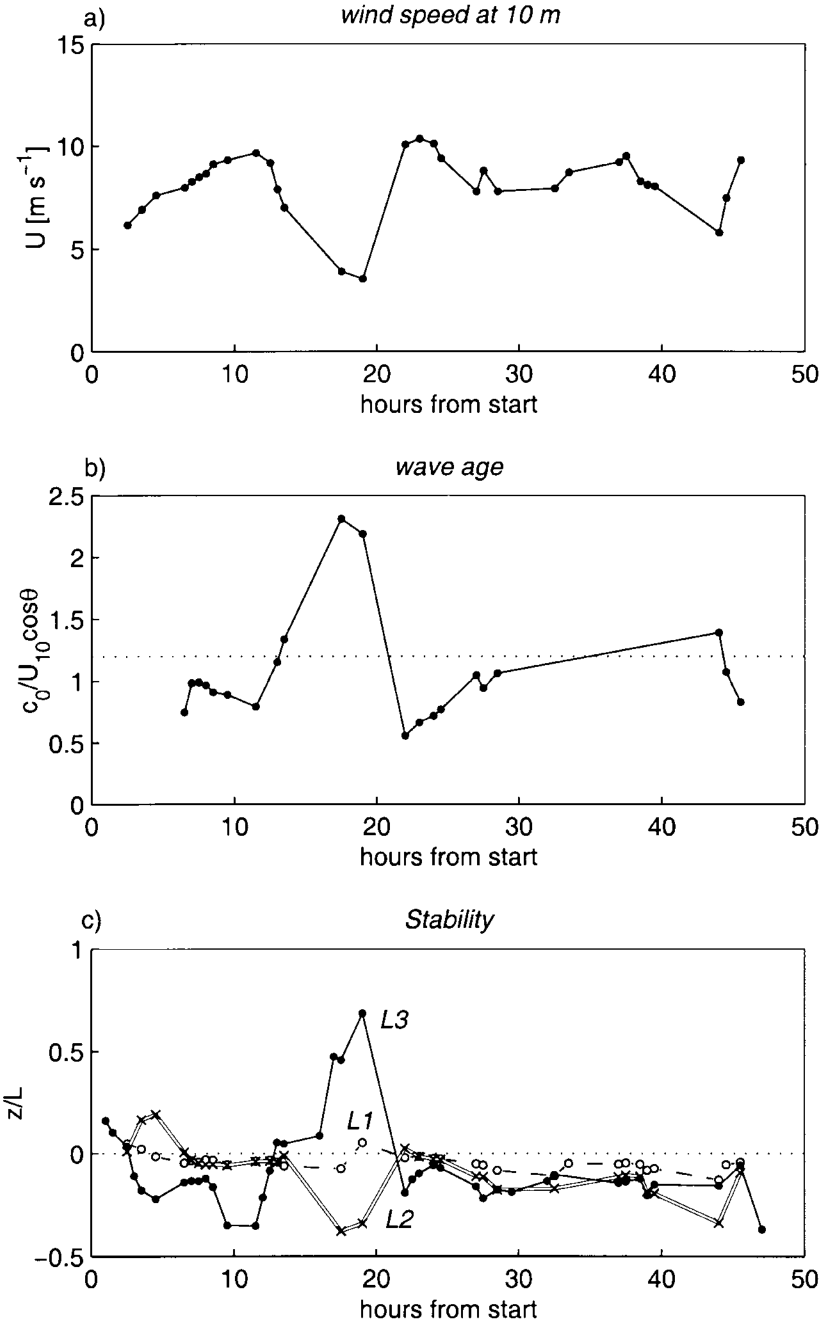

Figure 9. General conditions for 25–26 August 1996. The x-axis shows hours from August 25, 0000 LST, (a) wind speed at 10 m, (b) wave age $c_0/(U_{10}\cos\theta)$, (c) stability z/L (symbols as in Figure 4).

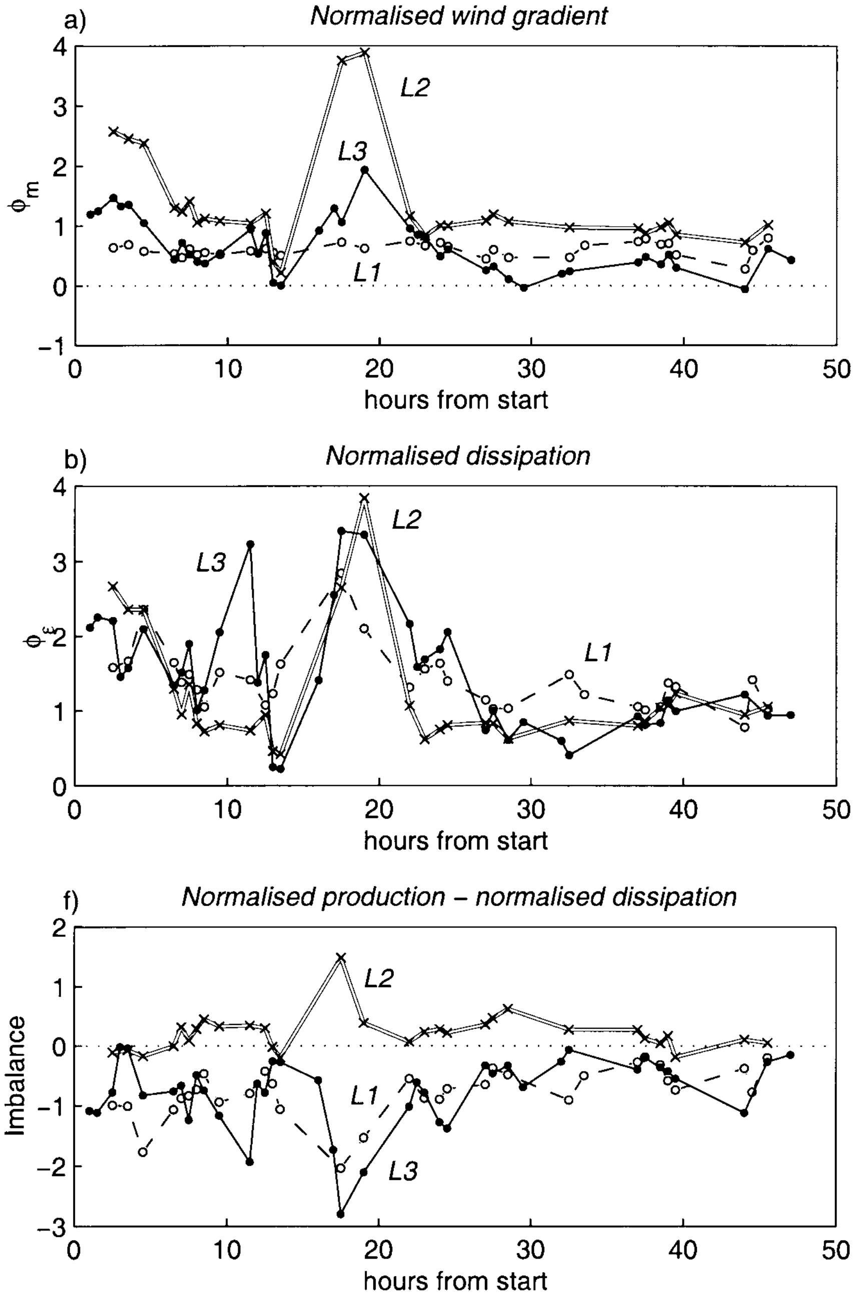

Figure 10. Turbulent parameters for 25–26 August 1996. The x-axis shows hours from August 25, 0000 LST, (a) normalised wind gradient, (b) normalised dissipation and (c) imbalance between normalised production and dissipation. Symbols as in Figure 4.

1 shows ϕ_m slightly less than 1.0 during the whole period, which is as expected when considering the stability (Figure 3) and the fact that the swell is not *very* strong, which then would give lower ϕ_m.

The normalised dissipation, ϕ_ϵ (Figure 10b), does not show the same clear distinction between the three levels as ϕ_m, even if some differences can be found. This again agrees well with Section 3.4.2. where it was found that ϕ_ϵ is only a function of *z/L*, except during strong swell, when the actual height, *z*, in addition to *z/L*, has to be taken into account.

The behaviour of ϕ_m and ϕ_ϵ is reflected in Figure 10c, where the imbalance between normalised production and normalised dissipation (i.e., the sum of the transport terms) is shown. The imbalance at Level 2 is close to zero or positive during the whole period with the largest positive imbalance occurring during the swell period (12–20 h). The imbalance at Levels 1 and 3 is quite close in magnitude even if Level 3 is more scattered than Level 1. In contrast to Level 2, Levels 1 and 3 are negative, i.e., dissipation exceeding production during the whole period. This again suggests the idea that Level 2 most often is in the transition layer, and supports the findings in Section 4.3.

To conclude, this detailed study of two days with changing wind speeds and wage ages supports the results from the long term study in Sections 3 and 4. Thus, it must be emphasised again that the measurement height has to be accounted for, in addition to the stability and the wave age.

6. Discussion and Conclusions

It has been shown that waves play an important role in the atmospheric boundary layer over the sea, and that some turbulence parameters have a strong dependence on height due to the wave state.

During neutral conditions, the normalised wind gradient ϕ_m has a height dependency that can be divided into three height intervals (cf. Figure 2): A lower layer that is directly influenced by the waves, a middle transition layer and a higher undisturbed, ‘ordinary’ surface layer. In the transition layer the wind profile becomes ‘too steep’ before returning to ‘normal’ in a layer higher up. The depth of these layers is a strong function of the wave state, but how to exactly determine these depths is not completely clear.

The lowest measuring level (Level 1, about 10 m), is in the wave disturbed layer on average. For neutral conditions, ϕ_m is close to 1.0, but for unstable conditions, ϕ_m will become much smaller than over land. The middle level (Level 2, about 18 m), is often in the transition layer, giving a higher value of ϕ_m than that is commonly assumed – during neutral conditions about 1.5 instead of 1.0; the transition layer exists already for saturated waves, i.e., about $c_0/(U_{10}\cos\theta) > 0.5$. The highest level (Level 3, about 26 m), is mostly in the undisturbed, ‘ordinary’ surface layer above the transition layer, giving ϕ_m close to 1.0 for neutral conditions.

The dissipation, ϕ_ϵ, is not as dependent on the actual measurement height in near-neutral conditions as ϕ_m, at least in no-swell conditions, i.e., the inertial subrange scales with height. The reason for this is not completely clear, but as showed by Rieder and Smith (1998), the inertial subrange does not react as the whole spectrum, and most of the swell influence is contained in frequencies between 0.06–0.16 Hz. The inertial subrange is normally located at higher frequencies. Since the dissipation has been determined from the inertial subrange, it might be possible that ϕ_ϵ is not as influenced by swell as ϕ_m, i.e., the influence starts to appear first at $c_0/(U_{10}\cos\theta) \approx 0.9$.

This difference between ϕ_m and ϕ_ϵ will, of course, also influence the balance in the TKE budget, and therefore also the inertial dissipation method. The height dependence of the imbalance between production and dissipation will be a strong function of stability and wave age. Inertial dissipation measurements that are performed with classical formulations in the transition layer will probably give an average value close to zero or even positive (i.e., production exceeds dissipation).

A balance between production and dissipation for neutral conditions was, for example, found by Dupuis et al. (1997), who performed measurements at about 16 m above the sea surface with the inertial dissipation method. That production exceeded dissipation for most conditions was also found by Yelland and Taylor (1996) from measurements at 16 and 18.5 m. They used an effective value of the Kolmogorov constant of 0.55 (Equation (4)), which, compared to this study, implies that the curves in Figures 7 and 8 move upwards towards more positive values.

Thus, it might be possible that these experiments were performed in the transition layer and thereby have a balance between production and dissipation that is not a complete description of the whole surface layer. Completely different parameterisations have to be used depending on the measurement height. If a buoy is used, the measurements are probably within the wave influenced layer, but if a ship is used it is more uncertain in which layer the measurements are taking place.

To conclude, the height of the measurements has to be considered when measurements are made in the atmospheric boundary layer over the sea. This height dependence can maybe explain why earlier results regarding the TKE budget are somewhat inconclusive. The problem could perhaps be solved by having a measurement height high enough to be outside the transition layer, but there remains uncertainty as to whether that height is still within the surface layer. Also, the wave influence can reach throughout the whole boundary layer during swell (e.g., Smedman et al., 1994). Another solution is to redefine the parameterisations used to fit the specific layer, but that would require wave measurements and a more complete definition of the depth of the different layers.

Acknowledgements

This work has been performed within the EU-funded project AutoFlux (contract MAS3-CT97-0108). The authors would like to thank Dr. Hans Bergström and Dr. Mikael Magnusson for help with the data and members of the MIUU staff for participation in the Östergarnsholm field campaigns. Dr. Kimmo Kahma and Dr. Heidi Pettersson at FIMR are acknowledged for the wave measurements, and Barry Broman at SMHI is acknowledged for the sea-level measurements at Visby. Thanks are also given to Prof. em. Ulf Högström for valuable comments on the manuscript.

References

Deacon, E. L.: 1988, 'The Streamwise Kolmogoroff Constant', *Boundary-Layer Meteorol.* **42**, 9–17.

Dobson, F. W.: 1994, 'Measuring the Relationship between Wind Stress and Sea State in the Open Ocean in the Presence of Swell', *Atmosphere-Ocean* **32**, 237–256.

Drennan, W. M., Kahma, K. K., and Donelan, M. A.: 1999, 'On Momentum Flux and Velocity Spectra over Waves', *Boundary-Layer Meteorol.* **92**, 489–515.

Dupuis, H., Taylor, P. K., Weill, A., and Katsaros, K.: 1997, 'Inertial Dissipation Method Applied to Derive Turbulent Fluxes over the Ocean during the Surface of the Ocean, Fluxes and Interactions with the Atmosphere/Atlantic Stratocumulus Transition Experiment (SOFIA/ASTEX) and Structure des Echanges Mer-Atmosphere, Proprietes des Heterogeneites Oceaniques: Recherche Experimentale (SEMAPHORE) Experiments with Low to Moderate Wind Speeds', *J. Geophys. Res.* **102**, 21115–21129.

Edson, J. B. and Fairall, C. W.: 1998, 'Similarity Relationships in the Marine Atmospheric Surface Layer for Terms in the TKE and Scalar Variance Budgets', *J. Atmos. Sci.* **55**, 2311–2328.

Fairall, C. W. and Larsen, S. E.: 1986, 'Inertial-Dissipation Methods and Turbulent Fluxes at the Air-Ocean Interface', *Boundary-Layer Meteorol.* **34**, 287–301.

Grachev, A. A. and Fairall, C. W.: 2001, 'Upward Momentum Transfer in the Marine Boundary Layer', *J. Phys. Oceanog.* **31**, 1698–1711.

Grelle, A. and Lindroth, A.: 1994, 'Flow Distortion by a Solent Sonic Anemometer: Wind Tunnel Calibration and its Assessment for Flux Measurements over Forest and Field', *J. Atmos. Oceanic Tech.* **11**, 1529–1542.

Högström, U.: 1990, 'Analysis of Turbulence Structure in the Surface Layer with a Modified Similarity Formulation for Near Neutral Conditions', *J. Atmos. Sci.* **47**, 1949–1972.

Högström, U.: 1996, 'Review of Some Basic Characteristics of the Atmospheric Surface Layer', *Boundary-Layer Meteorol.* **78**, 215–246.

Janssen, P. A. E. M.: 1999, 'On the Effect of Ocean Waves on the Kinetic Energy Balance and Consequences for the Inertial Dissipation Method', *J. Phys. Oceanog.* **29**, 530–534.

Kaimal, J. C. and Gaynor, J. E.: 1991, 'Another Look at Sonic Thermometry', *Boundary-Layer Meteorol*. **56**, 401–410.

Lenschow, D. H.: 1974, 'Model of the Height Variation of the Turbulent Kinetic Energy Budget in the Unstable Planetary Boundary Layer', *J. Atmos. Sci.* **31**, 465–474.

Obukhov, A. M.: 1971, 'Turbulence in an Atmosphere with a Non-Uniform Temperature', *Boundary-Layer Meteorol.* **2**, 7–29.

Pierson Jr., W. J. and Moskowitz, L.: 1964, 'A Proposed Spectral Form for Fully Developed Wind Seas Based on the Similarity Theory of S. A. Kitaigorodskii', *J. Geophys. Res.* **69**, 5181–5190.

Rieder, K. F. and Smith, J. A.: 1998, 'Removing Wave Effects from the Wind Stress Vector', *J. Geophys. Res.* **103**, 1363–1374.

Rutgersson, A., Smedman, A., and Högström, U.: 2001, 'The Use of Conventional Stability Parameters Stability Parameters during Swell', *J. Geophys. Res.* **106**, 27117–27134.

Schacher, G. E., Davidson, K. L., Houlihan, T., and Fairall, C. W.: 1981, 'Measurements of the Rate of Dissipation of Turbulent Kinetic Energy, ϵ over the Ocean', *Boundary-Layer Meteorol*. **20**, 321–330.

Sjöblom, A. and Smedman, A.: 2002, 'The Turbulent Kinetic Energy Budget in the Marine Atmospheric Surface Layer', *J. Geophys. Res.* **107**(C10), 3142, doi: 10.1029/2001 JC 001016.

Smedman, A., Högström, U., Bergström, H., Rutgersson, A., Kahma, K. K., and Pettersson, H.: 1999, 'A Case Study of Air–Sea Interaction during Swell Conditions', *J. Geophys. Res.* **104**, 25833–25851.

Smedman, A., Tjernström, M., and Högström, U.: 1994, The Near-Neutral Marine Atmospheric Boundary Layer with No Surface Shearing Stress: A Case Study', *J. Atmos. Sci.* **51**, 3399–3411.

Wilczak, J. M., Edson, J. B., Højstrup, J., and Hara, T.: 1999, The Turbulent Kinetic Energy in the Marine Atmospheric Surface Layer', in G. L. Geernaert (ed.), *Air–Sea Exchange: Physics, Chemistry and Dynamics*, Kluwer Academic Publishers, Dordrecht, pp. 153–173.

Wyngaard, J. C. and Coté, O. R.: 1971, 'The Budgets of Turbulent Kinetic Energy and Temperature Variance in the Atmospheric Surface Layer', *J. Atmos. Sci.* **28**, 190–201.

Yelland, M. and Taylor, P. K.: 1996, 'Wind Stress Measurements from the Open Ocean', *J. Phys. Oceanog.* **26**, 541–558.